Research Square

Preprints are preliminary reports that have not undergone peer review.
They should not be considered conclusive, used to inform clinical practice,
or referenced by the media as validated information.

From QbD to Explainable AI: Predictive Design Space Mapping of Lecithin/Chitosan Nanoparticles

Dr. Rahul Dhaigude

rahul.dhaigude@sims.edu

Symbiosis Institute of Management Studies, Symbiosis International (Deemed University), Pune, India
https://orcid.org/0000-0003-3703-2690

Dr. Sonal Solanki

Hon. Shri Babanrao Pachpute Vichardhara Trust's Group of Institutions, Faculty of Pharmacy, Kashti, Ta-Shrigonda, Ahilyanagar, Maharastra, India, 414071 https://orcid.org/0009-0007-5535-3881

Dr. Nikunj Solanki

drnikunjsolanki@gmail.com

Hon. Shri Babanrao Pachpute Vichardhara Trust's Group of Institutions, Faculty of Pharmacy, Kashti, Ta-Shrigonda, Ahilyanagar, Maharastra, India, 414071 https://orcid.org/0009-0003-2271-9382

Dr. Sreekanth Thota

Vaagdevi College of Pharmacy Autonomous, Ramnagar, Hanamkonda, Telangana, India, 506001
https://orcid.org/0000-0002-7501-3987

Pranita Santosh Shankaratti

Dr. D. Y. Patil College of Pharmacy, Nigadi Pradhikaran, Akurdi, Pune, Maharastra, India 411044
https://orcid.org/0000-0002-7107-2226

Dr. Pallavi Chiprikar

Department of Basic Sciences, School of Sciences and Humanities, SR University, Warangal, India 506371 https://orcid.org/0000-0001-7333-5467

Research Article

Keywords: Explainable artificial intelligence, Quality by Design, Lecithin/chitosan nanoparticles, Machine learning, Predictive design space, Critical quality attributes

Posted Date: June 1st, 2026

DOI: https://doi.org/10.21203/rs.3.rs-9854829/v1

License: This work is licensed under a Creative Commons Attribution 4.0 International License.
Read Full License

Additional Declarations: The authors declare no competing interests.

From QbD to Explainable AI: Predictive Design Space Mapping of Lecithin/Chitosan Nanoparticles

Dr. Rahul Dhaigude[1], Dr. Sonal Solanki[2], Dr. Nikunj Solanki[2], Dr. Sreekanth Thota[3], Pranita Santosh Shankaratti[4], Dr. Pallavi Chiprikar[5]

1. Symbiosis Institute of Management Studies, Symbiosis International (Deemed University), Pune, India
2. Hon. Shri Babanrao Pachpute Vichardhara Trust's Group of Institutions, Faculty of Pharmacy, Kashti, Ta-Shrigonda, Ahilyanagar, Maharastra, India, 414071
3. Vaagdevi College of Pharmacy Autonomous, Ramnagar, Hanamkonda, Telangana, India, 506001
4. Dr. D. Y. Patil College of Pharmacy, Nigadi Pradhikaran, Akurdi, Pune, Maharastra, India 411044
5. Department of Basic Sciences, School of Sciences and Humanities, SR University, Warangal, India 506371

Corresponding Authors

Dr. Rahul Dhaigude- Email - rahul.dhaigude@sims.edu

Dr. Nikunj Solanki – Email – drnikunjsolanki@gmail.com

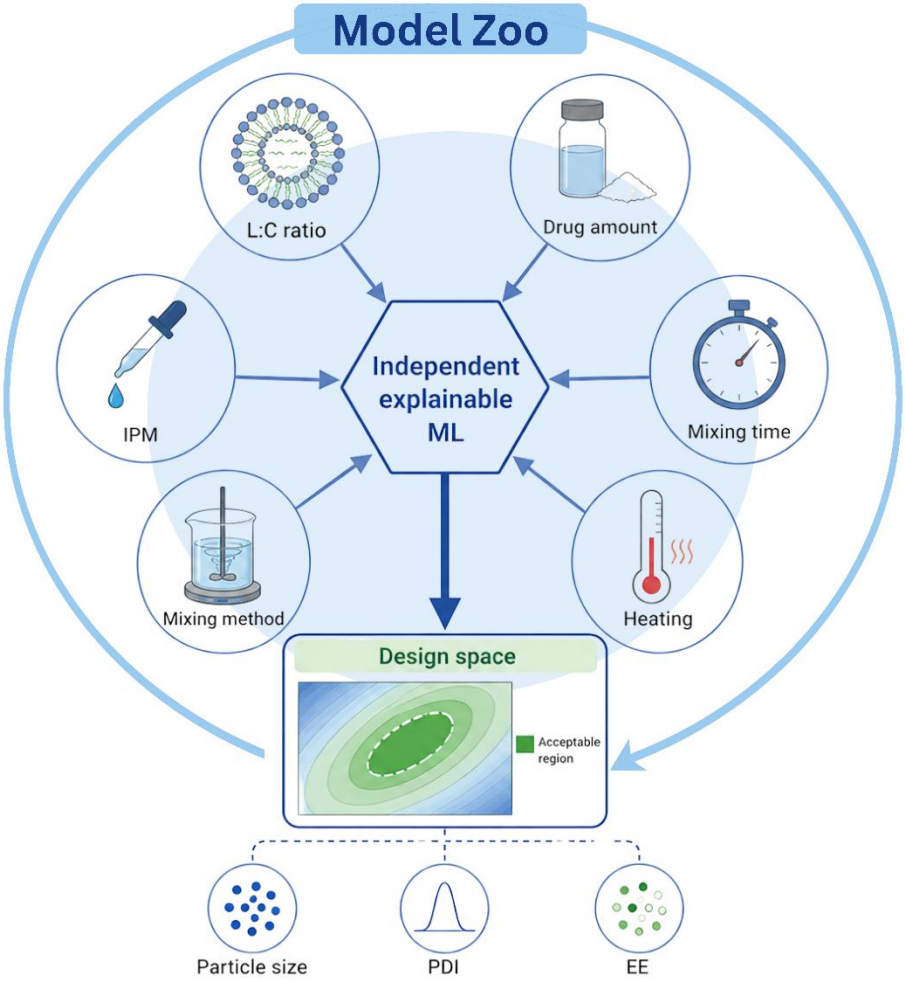
Abstract

Quality by Design (QbD) studies generate structured formulation datasets, but response surface models may not fully describe nonlinear or response-specific behavior in nanoparticle systems. This study reanalyzed a published silymarin-loaded lecithin/chitosan nanoparticle QbD dataset to determine whether independent explainable machine learning could add predictive and interpretive value to conventional QbD outputs. Twenty-nine formulation runs, comprising six formulation/process inputs and three critical quality attributes—particle size, polydispersity index (PDI), and entrapment efficiency—were extracted and modeled. A model-zoo of 105 regression variants per response was evaluated using leave-one-out cross-validation, followed by optimized-checkpoint comparison with reported QbD/RSM predictions, permutation feature importance, partial dependence analysis, and predictive design space mapping. Model performance was response dependent: XGBoost provided the best global particle-size prediction ($R^2 = 0.926$; RMSE = 27.52 nm), Extra Trees was best for PDI ($R^2 = 0.695$; RMSE = 0.0379), and distance-weighted KNN was best for entrapment efficiency ($R^2 = 0.938$; RMSE = 1.72%). At the optimized checkpoint, Gaussian Process regression predicted particle size with lower error than RSM (0.789 vs. 8.804 nm), and checkpoint-compatible Random Forest predicted PDI more closely than RSM (0.0004 vs. 0.032 absolute error), whereas RSM remained slightly closer for entrapment efficiency. Explainable AI identified lecithin:chitosan ratio and drug amount as recurring formulation drivers, while the predicted acceptable region was concentrated within intermediate formulation ranges. These findings support explainable machine learning as a complementary layer for QbD-based nanoparticle development rather than as a replacement for response surface modeling.

Keywords:

Explainable artificial intelligence; Quality by Design; Lecithin/chitosan nanoparticles; Machine learning; Predictive design space; Critical quality attributes

Graphical abstract:



Introduction

Lecithin/chitosan nanoparticles are self-assembled colloidal carriers formed through interactions between negatively charged phospholipid groups of lecithin and protonated amino groups of chitosan [1,2]. This carrier system is relevant for poorly water-soluble drugs because lecithin can provide a lipidic environment for hydrophobic molecules, whereas chitosan contributes cationic charge, mucoadhesive behavior, and colloidal stabilization [3,4]. However, the final properties of these nanoparticles are strongly influenced by formulation composition and processing conditions [1,2]. Variables such as lecithin:chitosan ratio, drug amount, mixing method, mixing time, heating, and lipidic solubilizer use can affect particle formation, aggregation behavior, size distribution, and drug entrapment [2,5]. Therefore, lecithin/chitosan nanoparticles provide a suitable formulation system for evaluating how data-driven methods can support the interpretation of formulation behavior.

Quality by Design (QbD) provides a systematic framework for linking formulation and process variables with critical quality attributes [6,7]. In nanoparticle development, particle size, polydispersity index (PDI), and entrapment efficiency are commonly monitored because they influence dispersion quality, physical stability, drug loading, and formulation reproducibility [7,8]. Response surface methodology (RSM) is frequently used in QbD studies because it provides mathematical equations, response plots, and optimized factor settings [6,9]. These features make RSM useful when the number of experimental batches is limited. At the same time, RSM generally depends on a predefined polynomial structure. If formulation behavior is nonlinear, local, or controlled by complex interactions, a single polynomial model may not fully describe the experimental response.

Dawoud et al. [5] reported the development of silymarin-loaded lecithin/chitosan nanoparticles by integrating QbD with artificial intelligence. In that study, I-optimal screening was used to evaluate six formulation and process variables, and D-optimal design was subsequently used to optimize lecithin:chitosan ratio and drug amount. The optimized formulation showed nanosized particles with low PDI and high entrapment efficiency. The authors also applied artificial neural network modeling mainly for prediction of drug release at selected time points [5]. Their work provided an important example of how QbD and AI can be combined in nanoparticle formulation development.

Although that study established a useful experimental and computational benchmark, it also leaves an important question for further investigation. The AI component was primarily based on neural network modeling and was focused on release prediction [5]. Less attention was given to whether other machine-learning algorithms could predict the main QbD-related quality attributes, namely particle size, PDI, and entrapment efficiency, while also explaining the contribution of each formulation variable [10,11]. This distinction is important because neural networks may perform well for prediction but are often less transparent [10,12]. For small tabular formulation datasets, alternative methods such as gradient boosting, extra trees, support vector regression, kernel ridge regression, Gaussian process regression, k-nearest neighbors, and explainable boosting models may be appropriate depending on the response being modeled [10,13].

The present study used this published dataset rather than generating a new wet-laboratory dataset. This choice was deliberate. The aim was not to reproduce the original formulation experiment, but to reanalyze an available QbD dataset using independent explainable machine-learning methods. Repeating the same experimental study would require new materials, solvents, instruments, and analytical resources, while also introducing variability due to differences in material batch,

laboratory environment, and processing conditions. Such repetition is important when experimental confirmation is required, but it is not necessary for initial benchmarking of computational methods on an already reported dataset. A published dataset also provides a transparent reference point because the original QbD predictions, optimized formulation, and observed checkpoint values are available for comparison.

Use of published formulation data is also relevant from sustainability and reproducibility perspectives [10,13]. Many QbD studies are designed to reduce experimental burden while still generating structured data. These datasets are often underused after the original optimization is completed. Reanalysis of such data can help determine whether additional information can be extracted without immediate repetition of laboratory work [10]. It also allows different algorithms to be compared under the same data conditions. If a computational workflow shows value during secondary analysis, future experimental studies can be planned more efficiently, with fewer unnecessary batches and clearer confirmatory objectives.

This type of analysis is increasingly relevant because pharmaceutical development is moving toward digital and model-informed workflows [10,14]. However, the use of AI in formulation science requires careful validation. Small DoE datasets are valuable but are also vulnerable to overfitting when complex models are used without appropriate validation [11,13]. A high training fit alone does not establish that a model is useful. The model must be evaluated using a validation strategy suitable for small datasets and should generate outputs that can be interpreted in formulation terms [15,16]. Explainable AI can help meet this need by identifying the relative importance of formulation variables and by showing how important variables influence predicted responses across the design region [10,14].

The aim of the present study was to develop an independent explainable machine-learning workflow for predictive design space mapping of lecithin/chitosan nanoparticles using the published QbD dataset. The specific objectives were to extract and preprocess the reported formulation data, train a broad model-zoo for particle size, PDI, and entrapment efficiency [10,13], validate model performance using leave-one-out cross-validation [16,17], compare selected AI predictions with the reported QbD/RSM predictions at the optimized formulation checkpoint, and interpret the selected models using explainable AI tools. In addition, AI-based digital design space maps were generated to visualize formulation regions predicted to satisfy predefined criteria for all three critical quality attributes.

This work does not claim that AI universally replaces QbD or that machine learning is superior for every nanoparticle response. Instead, it examines where independent explainable AI can add value to an existing QbD dataset. By combining model comparison, checkpoint evaluation, feature-importance analysis, partial-dependence interpretation, and predictive design space mapping, the study moves from black-box prediction toward a more transparent computational framework for formulation understanding.

2. Materials and Methods

2.1. Study Design and Data Source

This study was conducted as a secondary computational reanalysis of a published lecithin/chitosan nanoparticle formulation dataset [5]. The dataset was selected because it contained structured Quality by Design experimental data, measured critical quality attributes, and a reported optimized formulation checkpoint. No new wet-laboratory experiments were performed.

The source dataset included formulation runs generated during the screening and optimization of silymarin-loaded lecithin/chitosan nanoparticles. Data from the reported I-optimal screening design and D-optimal optimization design were extracted and combined into a single model-ready dataset. The optimized formulation reported in the source study was not used as a training point during model development. It was retained separately as a checkpoint for comparing independent machine-learning predictions with the reported response surface methodology predictions.

The computational workflow consisted of data extraction, data preprocessing, model-zoo construction, cross-validated prediction, model ranking, optimized-checkpoint comparison, explainable AI analysis, and predictive design space mapping [10,13]. The purpose of the analysis was to determine whether independent explainable machine-learning models could provide useful prediction and interpretation of nanoparticle critical quality attributes using the published QbD data [11,14].

2.2. Variables and Prediction Targets

Six formulation and process variables were used as model inputs: lecithin:chitosan molar ratio, drug amount, mixing time, heating condition, mixing method, and isopropyl myristate condition [5]. Lecithin:chitosan molar ratio, drug amount, and mixing time were treated as continuous numerical variables. Heating condition, mixing method, and isopropyl myristate condition were treated as categorical variables and encoded as binary numerical inputs.

Three critical quality attributes were used as prediction targets: particle size, polydispersity index, and entrapment efficiency. Particle size was modeled in nanometers, PDI as a dimensionless value, and entrapment efficiency as percentage drug entrapment. These responses were selected because they were consistently reported across the formulation dataset and were directly related to nanoparticle optimization.

Each response was modeled independently. This response-wise strategy was used because particle size, PDI, and entrapment efficiency may be influenced by different physicochemical and process-dependent mechanisms [6,10].

2.3. Data Extraction and Preprocessing

The reported formulation tables were extracted into a structured spreadsheet [5]. Each formulation run was entered as one row, with formulation and process variables as input columns and measured critical quality attributes as response columns [7,8]. When responses were reported as mean ± standard deviation, only the mean value was used for model development [18]. Standard deviation values were not modeled because the present analysis focused on prediction of the central experimental response.

Categorical variables were encoded before model training [15,19]. Heating was coded as 0 for absent and 1 for present. Mixing method was coded as 0 for mechanical stirring and 1 for sonication. Isopropyl myristate was coded as 0 for absent and 1 for present. Continuous variables were retained in their original experimental units.

The cleaned dataset contained 29 formulation runs and six input variables. Rows with incomplete input or response values were excluded before analysis. No missing-value imputation was applied. The final feature matrix was defined as X with 29 rows and 6 columns. Separate response vectors were prepared for particle size, PDI, and entrapment efficiency.

2.4. Computational Workflow

The computational workflow was implemented as a reproducible Python notebook [18]. The same cleaned dataset, input variables, validation method, and performance metrics were used for all candidate models. The workflow was organized into six main steps: model-zoo construction, leave-one-out cross-validation [17], model ranking, optimized-checkpoint comparison, explainable AI analysis, and design space mapping.

The independent machine-learning models were trained directly on the observed experimental responses. The reported RSM equations were not used as input features, and RSM-predicted values were not used as training targets. This ensured that the machine-learning models remained independent of the original QbD mathematical models.

All scale-sensitive models were implemented within preprocessing pipelines so that standardization was applied only within the appropriate training fold during cross-validation. This procedure was used to reduce the risk of data leakage between training and test samples [13].

2.5. Machine-Learning Models

A model-zoo approach was used to compare multiple machine-learning algorithms under the same validation conditions [10,13]. The candidate models included polynomial ridge regression, Bayesian ridge regression, k-nearest neighbors regression, support vector regression with radial basis function kernel, kernel ridge regression, random forest regression, extra trees regression, gradient boosting regression, histogram gradient boosting regression, Gaussian process regression, XGBoost, CatBoost, LightGBM, explainable boosting machine, voting ensemble, and stacked ensemble models [14,18].

Several hyperparameter variants were evaluated for selected model families. Different values of k were tested for KNN. Multiple regularization and kernel settings were tested for support vector regression and kernel ridge regression. Different tree depths, learning rates, and leaf settings were evaluated for boosting and ensemble models.

Each candidate model was trained separately for particle size, PDI, and entrapment efficiency [5,10]. This approach allowed the best-performing algorithm to be selected independently for each response rather than forcing one model structure across all critical quality attributes.

2.6. Cross-Validation and Performance Metrics

Leave-one-out cross-validation was used for model evaluation. This method was selected because the dataset was small and each formulation run was valuable for estimating predictive performance. In each iteration, one formulation run was held out as the test sample, and the remaining runs were used for model training. The procedure was repeated until each run had been used once as the test sample.

Cross-validated predictions were compared with the observed experimental responses. Model performance was quantified using the coefficient of determination (R^2), mean absolute error, and root mean squared error [20,21]. RMSE was used as the primary ranking metric because it penalizes larger prediction errors [22,23]. MAE was used to express the average prediction error in the original response unit [18,21]. R^2 was used to describe the proportion of variance explained by the cross-validated predictions.

The same cross-validation procedure and performance metrics were applied to all models and all responses to allow direct comparison of algorithm performance.

2.7. Model Selection

Model selection was performed separately for each response. First, the primary internally validated model was selected as the model with the lowest leave-one-out cross-validated RMSE [17,18]. This selection reflected the strongest overall predictive performance and accuracy within the available small dataset [20,24].

Second, a checkpoint-compatible selection was performed for comparison with the reported optimized formulation [5]. Candidate models were restricted to those with acceptable cross-validated performance, defined as RMSE not more than 30% higher than the best RMSE for that response [25,26]. Within this candidate pool, the model with the lowest absolute prediction error at the optimized formulation checkpoint was selected to evaluate local accuracy at the target region.

This two-level strategy was used to avoid selecting a model only because it matched a single checkpoint, which can be a risk in small datasets [27,28]. The optimized formulation was not used for model training, cross-validation, or hyperparameter tuning. It was used only after model evaluation as an external comparison point to assess the model's reliability for the specific optimization target.

2.8. Optimized Checkpoint Comparison

The selected independent AI models were compared with the reported QbD/RSM prediction at the optimized formulation checkpoint. The checkpoint formulation had a lecithin:chitosan molar ratio of 18.331 and drug amount of 38.354 mg, with process variables fixed at the reported optimized preparation condition.

For each response, the reported observed optimized-batch value was used as the reference [5,29]. Absolute prediction error was calculated for both the reported RSM prediction and the selected AI prediction. The method with the smaller absolute error was considered closer to the observed checkpoint value [5,6].

This comparison was limited to particle size, PDI, and entrapment efficiency [5,30]. It was not interpreted as a direct comparison with the artificial neural network release model reported in the source study, because the present analysis modeled nanoparticle quality attributes rather than drug-release endpoints.

2.9. Explainable AI

Explainable AI analysis was performed for the final selected models [10,13]. Permutation feature importance was used as the primary model-independent explanation method [31,32]. In this method, each input variable was randomly permuted while the remaining variables were kept unchanged. The increase in prediction error after permutation was used as the importance score for that variable.

Partial dependence analysis was performed for the most important variables identified for each response. For each selected variable, values were varied across the observed experimental range, and the average model prediction was calculated while the remaining variables were retained in the dataset. Partial dependence plots were generated separately for particle size, PDI, and entrapment efficiency.

The explainability analysis was used to determine whether the selected models identified formulation variables that were scientifically plausible and relevant to nanoparticle formation. The

purpose was not only to explain model output, but also to connect model behavior with formulation interpretation [10,13].

2.10. Predictive Design Space

Predictive design space mapping was performed using the final selected independent AI models [10,13]. Lecithin:chitosan molar ratio and drug amount were varied across the studied experimental range to generate a two-dimensional prediction grid. The remaining process variables were fixed at the favorable preparation setting identified in the source study: short mixing time, absence of heating, mechanical stirring, and presence of isopropyl myristate.

At each grid point, the selected AI models predicted particle size, PDI, and entrapment efficiency [10]. Individual response maps were generated for the three quality attributes. A combined acceptable region was then identified using predefined criteria: particle size ≤ 200 nm, PDI ≤ 0.30, and entrapment efficiency $\geq 90\%$ [5,29]. These thresholds were selected based on the optimal ranges reported for stable, monodisperse, and high-capacity lecithin/chitosan nanocarriers.

Grid points satisfying all three criteria were classified as acceptable [7,29]. The resulting map was interpreted as a computationally predicted operating region. It was not treated as a confirmed regulatory design space because no new confirmatory batches were prepared in the present study.

2.11. Software and Reproducibility

All analyses were performed in Python using a Jupyter Notebook environment to ensure transparency and iterative documentation. This approach follows established practices for reproducible research in computational drug development [33]. Machine-learning models were implemented primarily using the scikit-learn library, with advanced boosting algorithms implemented through XGBoost and LightGBM. The workflow integrated model interpretation methods to support explanation of the selected machine-learning pipelines and to provide formulation-relevant insights [34,35].

The computational pipeline was structured to automate key steps, including data preprocessing, model selection, and results analysis [35]. Figures were generated to visualize model performance and the resulting design space [18,36]. To maintain reproducibility across different software environments, sharing the programming code used for numerical calculations has become an essential standard in the field [33].

The notebook-based workflow was designed so that the full analysis could be rerun from the extracted dataset without manual intervention after data loading. By automating model construction and prediction from the formulation dataset, this workflow allowed systematic comparison of candidate pipelines within a defined search space [35]. Consistent use of fixed parameters and documented code supported the reliability and reusability of the computational analysis [33].

3. Results

3.1. Dataset Summary

The final model-ready dataset contained 29 experimental formulation runs extracted from the published lecithin/chitosan nanoparticle study. The dataset included 13 screening runs and 16 optimization runs. Six variables were used as model inputs: lecithin:chitosan molar ratio, drug amount, mixing time, heating condition, mixing method, and isopropyl myristate condition.

Particle size, polydispersity index, and entrapment efficiency were defined as the primary prediction targets [5,29]. The dataset structure, variable type, coding, and response units are summarized in Table 1.

The extracted dataset covered a broad experimental range suitable for comparative machine-learning evaluation. Lecithin:chitosan molar ratio ranged from 10 to 40, drug amount from 10 to 100 mg, and mixing time from 5 to 30 min. The observed responses also showed clear variation: particle size ranged from 131.8 to 499.9 nm, PDI from 0.132 to 0.400, and entrapment efficiency from 72.28 to 97.09%. These ranges provided adequate response variation for model comparison while representing a small Quality by Design-derived formulation dataset [5,7].

Categorical variables were encoded as binary inputs before modeling [15,19]. Heating, sonication, and IPM addition were therefore evaluated as discrete features alongside the numerical formulation variables within the same feature matrix [5]. This structure allowed the simultaneous assessment of composition and process-related effects on nanoparticle quality attributes [5,11].

3.2. Model Performance

A total of 105 independent model variants were evaluated for each response using leave-one-out cross-validation, giving 315 model-response comparisons. The tested algorithms included regression, kernel-based, distance-based, tree-based, boosting-based, probabilistic, and ensemble models. The complete model-zoo results are provided in Supplementary Table S1, and the top-ranked models by cross-validated RMSE are shown in Fig. 1.

For particle size, the best internally validated model was XGBoost with maximum depth 3 and learning rate 0.06. This model produced an LOOCV R^2 of 0.926, MAE of 17.09 nm, and RMSE of 27.52 nm (Table 2). The cross-validated performance indicates that the model captured major trends in particle-size variation across the formulation dataset.

For PDI, the best internally validated model was Extra Trees regression using all input features. This model produced an LOOCV R^2 of 0.695, MAE of 0.0281, and RMSE of 0.0379 (Table 2). The lower R^2 compared with particle size and entrapment efficiency should be interpreted together with the absolute error because PDI had a narrower numerical range and smaller response differences.

For entrapment efficiency, the best internally validated model was KNN regression with two neighbors and distance weighting. This model gave an LOOCV R^2 of 0.938, MAE of 1.16%, and RMSE of 1.72% (Table 2). The result indicates that entrapment efficiency was predicted with low absolute error using the selected distance-based model.

3.3. Final Model Selection

Model selection was evaluated at two levels to balance global predictive performance with local accuracy near the optimized formulation region. First, the primary model for each response was identified by the lowest leave-one-out cross-validation RMSE, reflecting the strongest overall performance within the available 29-run dataset. Second, optimized-checkpoint agreement was examined to determine whether models with acceptable global performance could predict the reported optimized batch more closely than the Quality by Design response surface methodology model. The final model-selection summary is presented in Table 3.

Based on the primary internal validation criterion, the top-performing global models were XGBoost for particle size, Extra Trees for PDI, and k-nearest neighbors for entrapment efficiency

(Table 3). These algorithms represented the most robust predictors across the full experimental design space. However, the model with the lowest overall RMSE was not always the most accurate at the specific optimized-checkpoint formulation. This was particularly evident for particle size, where XGBoost achieved the highest global R^2 but overpredicted the response at the optimized coordinates.

The checkpoint audit identified Gaussian Process regression as a more balanced model for particle-size prediction in the optimized region. It maintained acceptable cross-validated performance, with an LOOCV R^2 of 0.874, MAE of 22.19 nm, and RMSE of 35.80 nm, and predicted the optimized particle size with an absolute error of 0.79 nm (Table 3). For PDI, Random Forest with a minimum leaf size of three provided a checkpoint-compatible prediction while retaining acceptable validation performance. For entrapment efficiency, KNN with $k = 2$ remained the most robust model based on global validation.

These findings show that selecting models only by the lowest global RMSE can overlook candidates that perform better near the optimized operating region. Therefore, both cross-validated metrics and optimized-checkpoint agreement were considered during final interpretation.

3.4. Comparison with QbD Model

The independent AI predictions were compared with the reported Quality by Design response surface methodology predictions at the optimized formulation checkpoint to evaluate response-specific agreement with the observed optimized batch [5,37]. The observed optimized-batch values from the source study were 161.401 nm for particle size, 0.204 for PDI, and 97.060% for entrapment efficiency. The corresponding reported QbD/RSM predictions were 152.597 nm, 0.172, and 96.016%, respectively (Table 4).

For particle size, the reported QbD/RSM prediction showed an absolute error of 8.804 nm. In comparison, the lowest-error AI checkpoint prediction was obtained with Gaussian Process regression, which predicted 162.190 nm and showed an absolute error of 0.789 nm (Table 4). This represented a lower optimized-checkpoint error than the reported RSM value. Importantly, this Gaussian Process model also retained acceptable cross-validated performance across the full 29-run dataset, unlike some polynomial or kernel-based models that showed low checkpoint error but weak global validation.

For PDI, the reported QbD/RSM prediction had an absolute error of 0.032. A large proportion of the tested AI models, 88 out of 105, predicted the optimized PDI more closely than RSM. The checkpoint-compatible Random Forest model predicted 0.2044, giving an absolute error of 0.0004 (Table 4). This was the clearest AI improvement over the reported RSM prediction at the optimized checkpoint.

For entrapment efficiency, the reported QbD/RSM prediction showed an absolute error of 1.044%. The best globally validated AI model, KNN with two neighbors, predicted 95.564%, giving an absolute error of 1.496% (Table 4). In this case, RSM remained slightly closer to the observed value than the most robust cross-validated AI model. However, the full model audit indicated that some boosting variants, including LightGBM models, predicted optimized entrapment efficiency more closely than RSM but showed lower global cross-validated performance than KNN.

Across all 105 tested AI model variants, 10 models were closer than QbD/RSM for particle size, 88 for PDI, and 19 for entrapment efficiency (Table 4). These results indicate that AI performance was response dependent. Independent AI improved optimized-checkpoint prediction for particle

size and PDI when both checkpoint agreement and cross-validation were considered, whereas RSM remained slightly closer for entrapment efficiency.

3.5. Feature Importance

Permutation feature importance was calculated for the selected independent AI models to estimate the relative contribution of each input variable to model prediction. The importance profiles differed across particle size, PDI, and entrapment efficiency, indicating that the three responses were influenced by different combinations of formulation and process variables (Table 5 and Fig. 3).

For particle size, drug amount, lecithin:chitosan molar ratio, and mixing time showed the highest importance values, recorded at 44.95, 44.47, and 44.05, respectively (Table 5). In contrast, the binary process variables, including mixing method, heating, and IPM addition, showed lower importance scores. This indicates that particle-size prediction was mainly influenced by quantitative composition and processing duration.

For PDI, lecithin:chitosan molar ratio was the dominant variable, with a permutation importance value of 0.0419 (Table 5). Drug amount, heating, and IPM addition showed smaller contributions, while mixing method and mixing time had limited influence on model prediction. This suggests that the size-distribution response was mainly associated with the lecithin:chitosan balance in the selected model.

For entrapment efficiency, lecithin:chitosan molar ratio, mixing method, and drug amount were the three most important variables, with permutation importance values of 1.90, 1.87, and 1.81, respectively (Table 5). Mixing time and IPM addition showed secondary contributions, whereas heating had the lowest importance. This indicates that drug entrapment was influenced by both formulation composition and the method used for nanoparticle formation.

3.6. Partial Dependence Analysis

Partial dependence analysis was used to visualize the average direction of the main model-predicted effects. These plots were interpreted together with permutation feature importance because feature importance identifies influential variables, whereas partial dependence shows the direction and pattern of their effect (Fig. 4).

For particle size, lecithin:chitosan molar ratio showed a nonlinear effect. The predicted particle size was higher at the lower ratio region, decreased in the intermediate region, and increased again toward the higher end of the range (Fig. 4). Drug amount also showed a nonlinear response, with lower predicted particle size in the intermediate loading region. Mixing time showed a clear process effect, with longer mixing associated with higher predicted particle size.

For PDI, the partial dependence plot for lecithin:chitosan molar ratio showed lower predicted values in the intermediate ratio region and higher values toward the lower and higher ends of the range (Fig. 4). Drug amount had a smaller effect than lecithin:chitosan ratio, while heating produced only a limited average shift in predicted PDI.

For entrapment efficiency, the predicted response decreased with increasing lecithin:chitosan ratio and higher drug amount (Fig. 4). The mixing-method plot indicated lower predicted entrapment efficiency when sonication was used compared with mechanical stirring. These trends were consistent with the feature-importance results and supported the response-specific interpretation of the selected AI models.

3.7. Digital Design Space

Predictive design space maps were generated by varying lecithin:chitosan molar ratio and drug amount across the studied experimental range while fixing the remaining process variables at the favorable preparation conditions. These fixed conditions were short mixing time, absence of heating, mechanical stirring, and presence of isopropyl myristate. The individual response maps are shown in Fig. 5.

Across the generated prediction grid, the AI models predicted particle size values from 134.4 to 369.4 nm, PDI values from 0.193 to 0.343, and entrapment efficiency values from 83.71 to 97.07%. These predicted ranges were within the experimental response space and allowed simultaneous assessment of the three modeled critical quality attributes (Fig. 5).

The combined acceptable region was defined using predefined criteria: particle size $\leq$ 200 nm, PDI $\leq$ 0.30, and entrapment efficiency $\geq$ 90%. Under these criteria, 5,818 of 14,400 grid points were classified as acceptable, corresponding to 40.4% of the evaluated grid. The acceptable region was mainly concentrated within an intermediate formulation range, with lecithin:chitosan molar ratio approximately between 12.77 and 34.45 and drug amount approximately between 11.51 and 65.97 mg. The median acceptable point was close to a lecithin:chitosan ratio of 24.12 and a drug amount of 36.22 mg (Fig. 6).

The resulting digital design space should be interpreted as a computationally predicted operating region. It identifies formulation combinations expected to satisfy all three selected criteria, but it does not replace experimental confirmation or represent a validated regulatory design space.

3.8. Overall Model Interpretation

The independent AI analysis showed response-dependent model performance across the three nanoparticle quality attributes. Particle size and entrapment efficiency were predicted with strong cross-validated performance, whereas PDI showed moderate global performance but strong optimized-checkpoint agreement for several models (Tables 2–4). This indicates that each response had a different level of predictive difficulty within the same formulation dataset.

The comparison between global validation and optimized-checkpoint performance showed that model selection should not rely on R^2 or RMSE alone. Some AI models showed low checkpoint error despite poor cross-validated performance, indicating limited generalizability. Conversely, the best global model for particle size did not provide the closest optimized-checkpoint prediction. Gaussian Process regression provided a balanced particle-size result by combining good LOOCV performance with low checkpoint error (Tables 3 and 4).

The comparison with QbD/RSM was also response dependent. Independent AI improved optimized-checkpoint prediction for particle size when Gaussian Process regression was considered and clearly improved PDI prediction using the checkpoint-compatible Random Forest model. For entrapment efficiency, the most robust global AI model, KNN with two neighbors and distance weighting, was slightly less close than the reported RSM prediction, although some lower-ranked AI models showed closer local agreement (Table 4).

The explainability workflow identified lecithin:chitosan molar ratio and drug amount as recurring formulation drivers. Mixing time was more relevant for particle-size prediction, while mixing method was more relevant for entrapment efficiency. The digital design space translated these response-specific models into a visual operating region, where 40.4% of the evaluated grid satisfied the predefined criteria for all three responses (Figs. 3–6).

Overall, the results show that independent explainable AI can extract additional information from a published QbD dataset through model comparison, checkpoint-based evaluation, feature-level interpretation, and predictive design space mapping.

4. Discussion

The present study examined whether an independent explainable machine-learning workflow could extract additional predictive and interpretive value from a published QbD dataset of lecithin/chitosan nanoparticles [5]. The analysis was not designed to repeat the original experimental optimization or to replace the reported response surface model [5]. Instead, it was designed to test whether the same structured formulation dataset could support model comparison, response-wise prediction, optimized-checkpoint evaluation, and explainable design space mapping [10,13]. This distinction is important because the value of AI in small formulation datasets should not be judged only by whether one model gives a numerically closer prediction at one point [26,38]. A useful model should show reasonable performance across the dataset, should behave consistently at the optimized formulation, and should provide interpretation that is meaningful from a formulation perspective [24,38]. Recent reviews emphasize that while traditional Quality by Design is effective for simple systems, AI/ML methodologies are better suited for uncovering complex, high-dimensional, and non-linear relationships that often limit empirical and statistical approaches [10,39].

The model-zoo strategy showed that the best-performing algorithm depended on the response being modeled [18,40]. Particle size was best predicted globally by XGBoost, PDI by Extra Trees, and entrapment efficiency by distance-weighted KNN [18,41,42]. This response-specific behavior is expected because particle size, size distribution, and entrapment efficiency do not necessarily follow the same formulation logic [37,43]. Particle size is affected by particle formation, growth, aggregation, and dispersion energy [2,44]. PDI reflects the uniformity of the dispersed system and may be sensitive to small changes in particle population [37,44]. Entrapment efficiency depends on the interaction between the drug, lipidic phase, polymeric shell, and process conditions [5,45]. Therefore, forcing one algorithm to represent all responses would be less appropriate than selecting models independently for each CQA [10,13]. Other studies have similarly found that ensemble methods like XGBoost and AdaBoost often outperform single-algorithm approaches in predicting nanoparticle characteristics due to their ability to handle the "curse of dimensionality" in small datasets [42,46].

For particle size, the best global model was XGBoost, which showed strong leave-one-out cross-validated performance [18,47]. This suggests that nonlinear and interaction-based learning was useful for describing particle-size variation across the extracted dataset [43,47]. The superior performance of XGBoost in capturing critical manufacturing parameters from sparse experimental data has been noted in other colloidal systems, such as mRNA-lipid nanoparticles [48]. However, the optimized-checkpoint audit showed an additional important finding. Gaussian Process

regression predicted the optimized particle size more closely than the reported RSM prediction while also retaining acceptable cross-validated performance [5,26]. This is different from models that matched the checkpoint but performed poorly across the full dataset [24,28]. Some kernel ridge and polynomial ridge variants showed low checkpoint error but weak or negative cross-validated R^2 values, indicating poor generalizability [27,28]. These models should not be selected only because they matched one point. In contrast, Gaussian Process regression provided a better balance between global validation and local checkpoint agreement [5,38]. This supports its role as a checkpoint-compatible model for particle-size prediction, although the primary global model remained XGBoost [5,18].

The PDI result is particularly relevant because the independent AI models gave a much closer prediction at the optimized checkpoint than the reported RSM value [5,37]. Although the best PDI model showed only moderate cross-validated R^2, the absolute prediction error was small [37,44]. This highlights a common issue in modeling narrow-range responses: R^2 can appear modest even when the actual error is practically acceptable [43,46]. PDI values generally vary within a limited numerical range, and small experimental or instrumental differences can influence the statistical estimate of explained variance [40,44]. Therefore, interpretation of PDI models should consider MAE, RMSE, and checkpoint performance together [26,38]. The fact that many AI models predicted the optimized PDI more closely than RSM suggests that the PDI response may contain local nonlinear behavior that was not fully captured by the response surface equation [43,46]. Similar findings have identified that even with limited data points (e.g., n=72), explainable ML can significantly outperform traditional trial-and-error and simple statistical models in defining stability and uniformity of pharmaceutical suspensions [49].

Entrapment efficiency showed strong global prediction by KNN, indicating that formulations close to each other in input space had similar entrapment behavior [42,43]. This is plausible for a self-assembled colloidal system, where drug retention may depend on local similarity in lipid-polymer balance, drug loading, and dispersion method [45,50]. At the optimized checkpoint, however, the reported RSM prediction remained slightly closer than the most robust AI model [5]. This does not weaken the AI analysis because the difference was small and both methods predicted high entrapment efficiency [5]. It rather shows that AI superiority is response dependent [43,46]. In some cases, the conventional QbD/RSM equation may remain highly competitive, especially when the experimental response is well represented by the selected polynomial model [7,10]. Recent frameworks like TuNa-AI suggest that hybrid models coupling molecular feature learning with compositional inference can further enhance these outcomes by optimizing material selection and component ratios simultaneously [51].

A central message from these findings is that overfitting is not exclusive to machine learning [24,28]. Polynomial response surface models fitted to small DoE datasets can also show high internal R^2 values when multiple linear, interaction, quadratic, or higher-order terms are included [5]. Similarly, machine-learning models can appear highly accurate when judged only by one checkpoint or by training performance [27,38]. For this reason, the present study avoided relying

on a single indicator. The models were evaluated using leave-one-out cross-validation, error metrics, optimized-checkpoint comparison, and explainability outputs [17,18]. This combined evaluation is more informative than R^2 alone because it considers both global predictive stability and practical agreement near the optimized operating region [24,38]. The literature identifies that methodological flaws in many ML studies often stem from failing to use cross-validation or testing alternative models, emphasizing the need for the rigorous "model-zoo" approach used here [11].

The explainable AI results provided the main interpretive advantage of the workflow [10,13]. For particle size, drug amount, lecithin:chitosan molar ratio, and mixing time were the dominant variables [5,18]. The use of SHapley Additive exPlanations has become critical in the field to decompose predicted values into relative contributions for each input feature, moving beyond "black-box" predictions [18,49]. The partial dependence plots suggested nonlinear effects of both formulation ratio and drug amount, with more favorable particle-size predictions in an intermediate region [5]. This agrees with the expected behavior of self-assembled lecithin/chitosan nanoparticles [2,37]. At very low or very high compositional balance, incomplete stabilization, higher viscosity, or aggregation may increase particle size [37,44]. An intermediate ratio may provide better electrostatic balance between lecithin and chitosan, supporting more controlled particle formation [5]. The effect of mixing time also suggests that extended processing may increase particle collisions or structural rearrangement, contributing to larger particle size [5,44].

For PDI, lecithin:chitosan ratio was the most influential factor [5,37]. This supports the concept that the polymer-lipid balance is central to obtaining a uniform particle population [37,44]. If the ratio is not balanced, the system may contain particles with different degrees of chitosan association, leading to broader size distribution [5]. Drug amount had a smaller but detectable effect, suggesting that drug loading can influence dispersion uniformity, but not to the same extent as the structural balance between lecithin and chitosan [5]. For entrapment efficiency, lecithin:chitosan ratio, mixing method, and drug amount were the major variables [5,42]. The partial dependence plots indicated reduced entrapment at higher drug levels and under sonication [5]. This may reflect saturation of the lipid-polymer matrix or disruption of the forming nanoparticle structure during high-energy processing [42,43]. Such findings are corroborated by physics-informed ML frameworks which indicate that drug-polymer interactions and kinetic release are critical factors in encapsulation efficiency [52,53].

The predictive design space translated these response-specific models into a practical visual output [5,10]. By applying the criteria of particle size ≤ 200 nm, PDI ≤ 0.30, and entrapment efficiency $\geq 90\%$, the workflow identified a computationally acceptable region mainly within intermediate lecithin:chitosan ratio and drug amount [5,29]. This multi-objective visualization allows for the identification of optimal formulation "sweet spots" where competing CQAs can be satisfied simultaneously, a task traditionally limited by the linear nature of many response surface methods [39,46]. This supports the idea that balanced formulation composition is preferable to extreme factor settings when multiple CQAs must be controlled simultaneously [5,7]. In nanomedicine development, the "compositional window" often dictates stability; AI-guided mapping helps

visualize these boundaries with higher resolution than conventional DoE, particularly in high-dimensional spaces [7,11]. However, the map should be interpreted as a predictive computational design space, not as an experimentally confirmed regulatory design space [7,10]. Since the present work was a secondary analysis, additional confirmatory batches would be required before the predicted operating region could be used for formulation decision-making [18,42]. The transition from in silico predictions to validated commercial products requires a robust confirmation stage to account for batch-to-batch variability and scale-up effects [7,51].

The study has important limitations. The dataset was small and derived from a previously published study [5]. Although leave-one-out cross-validation is suitable for small datasets, it cannot fully replace prospective external validation [24,38]. Small datasets (e.g., $N < 100$) are susceptible to high variance in model performance; while cross-validation provides an estimate of generalizability, the true extrapolation risk often remains high without diverse external data [27,28]. The optimized formulation checkpoint provided a useful comparison point, but it represents only one external formulation condition [5]. Validating at a single point may result in a "local" fit that fails to capture the global behavior of the system, particularly when dealing with nonlinear effects of polymer concentrations or mixing speeds [26,50]. In addition, the present analysis focused on particle size, PDI, and entrapment efficiency [5]. It did not directly compare against the reported artificial neural network release model because release prediction involves a different endpoint and a different descriptor set [18,43]. Drug release is inherently time-dependent and often requires dynamic modeling or physics-informed AI approaches, which were beyond the scope of this static structural analysis [10,53]. Future work should reconstruct or generate a release dataset and compare explainable machine-learning models directly with ANN for release prediction [10,13].

Overall, the findings support the use of independent explainable machine learning as a complementary layer to QbD-based nanoparticle development [7,10]. The integration of AI does not necessitate the abandonment of QbD; rather, it strengthens it by providing a more granular understanding of critical material attributes and their interactions [39,52]. The analysis shows that AI can improve selected optimized-checkpoint predictions, especially for particle size and PDI, while RSM may remain competitive for other responses such as entrapment efficiency [5,46]. This suggests a hybrid approach where linear responses are handled by RSM and complex, high-energy process variables—such as those seen in microfluidic or ultrasonic manufacturing—are optimized through ensemble learning [13,48,51]. The main contribution of the workflow is not the claim that AI replaces QbD, but that it provides additional model comparison, validation, feature-level interpretation, and predictive design space visualization [18,42]. This multi-layered validation strategy—incorporating error metrics, checkpoint audits, and explainability—ensures that the resulting models are not just accurate, but also biologically and chemically plausible [11,41]. This balanced role is likely to be more useful for formulation development than a direct competition between AI and conventional QbD models [10,13]. Even with relatively sparse data points,

explainable ML can significantly outperform traditional trial-and-error in defining the stability and uniformity of complex pharmaceutical dispersions [45,49].

5. Conclusion

This study demonstrated that independent explainable machine learning can be used to reanalyze a published QbD dataset of lecithin/chitosan nanoparticles and generate predictive design space maps for key critical quality attributes. The model-zoo approach showed response-dependent performance. Particle size was best predicted globally by XGBoost, PDI by Extra Trees, and entrapment efficiency by distance-weighted KNN, indicating that a single algorithm was not optimal for all nanoparticle responses.

Comparison with the reported optimized formulation showed that independent AI improved selected checkpoint predictions. Gaussian Process regression provided a closer checkpoint-compatible prediction for particle size, while AI models predicted the optimized PDI more closely than the reported QbD/RSM model. For entrapment efficiency, the most robust AI model showed strong cross-validated performance, although the reported RSM prediction remained slightly closer at the optimized checkpoint. These findings indicate that AI should be considered as a complementary computational layer rather than a universal replacement for QbD/RSM.

The explainable AI analysis identified lecithin:chitosan molar ratio and drug amount as recurring formulation drivers. Mixing time contributed strongly to particle-size prediction, whereas mixing method was more relevant for entrapment efficiency. The predictive design space translated these response-specific models into an interpretable operating region for simultaneous control of particle size, PDI, and entrapment efficiency.

Overall, the study supports a balanced integration of QbD and explainable AI. Reanalysis of published formulation datasets can provide useful computational insight without unnecessary experimental repetition, provided that models are evaluated using cross-validation, checkpoint comparison, and interpretability rather than R^2 alone. Future work should include prospective experimental validation of the predicted operating region and direct comparison of explainable machine-learning models with neural-network-based release prediction.

6. References

1. Dmour, I. & Muti, H. Application of dual ionic/covalent crosslinking in lecithin/chitosan nanoparticles and their evaluation as drug delivery system. *Acta Pol. Pharm.* 78, 83–96 (2021).
2. Yousfan, A., Rubio, N., Natouf, A. H. *et al.* Preparation and characterisation of PHT-loaded chitosan lecithin nanoparticles for intranasal drug delivery to the brain. *RSC Adv.* 10, 28992–29009 (2020).
3. Clementino, A., Marchi, C., Pozzoli, M., Bernini, F. & Zimetti, F. Anti-inflammatory properties of statin-loaded biodegradable lecithin/chitosan nanoparticles: a step toward nose-to-brain treatment of neurodegenerative diseases. *Front. Pharmacol.* 12, 716380 (2021).
4. Clementino, A., Pellegrini, G., Banella, S. *et al.* Structure and fate of nanoparticles designed for the nasal delivery of poorly soluble drugs. *Mol. Pharmaceutics* 18, 3132–3146 (2021).
5. Dawoud, M., Mannaa, I. M., Abdel-Daim, A. & Sweed, N. M. Integrating artificial intelligence with Quality by Design in the formulation of lecithin/chitosan nanoparticles of a poorly water-soluble drug. *AAPS PharmSciTech* 24, 243 (2023).

6. Suriyaamporn, P., Pamornpathomkul, B., Wongprayoon, P. *et al.* The artificial intelligence and design of experiment assisted in the development of progesterone-loaded solid-lipid nanoparticles for transdermal drug delivery. *Pharmacia* 71, 1–12 (2024).
7. Maheshwari, R., Kapoor, D. U., Polaka, S. *et al.* Roadmap for commercial nanomedicine development: integrating Quality by Design principles with pharmaceutical nanotechnology. *Mol. Pharmaceutics* 22, 4337–4372 (2025).
8. Pandey, A., Karande, K. P., Sonawane, R. O. & Deshmukh, P. K. Applying quality by design (QbD) concept for fabrication of chitosan coated nanoliposomes. *J. Liposome Res.* 24, 37–52 (2013).
9. Agrawal, Y. & Goyal, M. Development and in vitro evaluation of nanoparticles of silymarin using central composite design. *Int. J. Res. Rev.* 10, 269–280 (2023).
10. Ros, H., Chan, N., Cook, M. T. & Shorthouse, D. Artificial intelligence and machine learning guided optimization in drug delivery. *Adv. Drug Deliv. Rev.* 232, 115781 (2026).
11. Fonseca, R., Lima, L. A., Gross, I. P. *et al.* The role of artificial intelligence and data science in nanoparticles development: a review. *Nanomedicine* 19, 1271–1283 (2024).
12. Palaniyappan, N., Nataraj, E., Thangamathesvaran, P. M. & Mathesan, R. AI-based prediction of particle size-dissolution relationships in solid and suspension dosage forms. *Int. J. Adv. Multidiscip. Res. Stud.* 6, 276–280 (2026).
13. Murray, J. D., Lange, J. J., Bennett-Lenane, H. *et al.* Advancing algorithmic drug product development: Recommendations for machine learning approaches in drug formulation. *Eur. J. Pharm. Sci.* 191, 106562 (2023).
14. Wu, Y. *et al.* Artificial intelligence for drug delivery: Yesterday, today and tomorrow. *Acta Pharm. Sin. B* 15, 1022 (2025).
15. Schmitt, J., Baumann, J. M. & Morgen, M. M. Predicting spray dried dispersion particle size via machine learning regression methods. *Pharm. Res.* 39, 3223–3239 (2022).
16. Bernau, C. R., Knödler, M., Emonts, J. & Jäpel, R. The use of predictive models to develop chromatography-based purification processes. *Front. Bioeng. Biotechnol.* 10, 1009102 (2022).
17. Li, R., Herreros, J. M., Tsolakis, A. & Yang, W. Machine learning-quantitative structure property relationship (ML-QSPR) method for fuel physicochemical properties prediction of multiple fuel types. *Fuel* 304, 121437 (2021).
18. Bannigan, P., Bao, Z., Hickman, R. J. *et al.* Machine learning models to accelerate the design of polymeric long-acting injectables. *Nat. Commun.* 14, 45 (2023).
19. Alqarni, M. & Alqarni, A. Development of several machine learning based models for determination of small molecule pharmaceutical solubility in binary solvents at different temperatures. *Sci. Rep.* 15, 8904 (2025).
20. Munir, N., Lima, T. d., Nugent, M. & McAfee, M. In-line NIR coupled with machine learning to predict mechanical properties and dissolution profile of PLA-Aspirin. *Funct. Compos. Mater.* 5, 12 (2024).
21. Muthudoss, P., Tewari, I. V., Rui, R. L. *et al.* Machine learning-enabled NIR spectroscopy in assessing powder blend uniformity: Clear-up disparities and biases induced by physical artefacts. *AAPS PharmSciTech* 23, 180 (2022).
22. Baum, M., Anders, D. & Reinicke, T. Optimizing injection molding simulations: comparative performance of Kriging and RSM surrogate models for process efficiency. *Discov. Mech. Eng.* 4, 8 (2025).

23. Galata, D. L., Domokos, A., Démuth, B. *et al.* In-line indirect concentration measurement of ultralow dose API during twin-screw wet granulation based on NIR and Raman spectroscopy. *Int. J. Pharm.* 664, 124650 (2024).
24. Majumdar, S. & Basak, S. C. Beware of external validation! - A comparative study of several validation techniques used in QSAR modelling. *Curr. Comput. Aided Drug Des.* 14, 284–291 (2018).
25. Ye, Z. & Ouyang, D. Prediction of small-molecule compound solubility in organic solvents by machine learning algorithms. *J. Cheminform.* 13, 75 (2021).
26. Rzewińska, A., Szlęk, J., Juszczyk, E. *et al.* Factors influencing the dispersibility of glycopyrronium bromide and indacaterol maleate – combined in vitro and in silico study. *AAPS PharmSciTech* 26, 92 (2025).
27. Rácz, A., Bajusz, D., Miranda-Quintana, R. A. & Héberger, K. Machine learning models for classification tasks related to drug safety. *Mol. Divers.* 25, 1409–1424 (2021).
28. Yan, F., Yu, M., Zhou, Y. & Wang, Q. A universal validation method for mitigating machine learning extrapolation risk. *Research Square* Preprint at https://doi.org/10.21203/rs.3.rs-3758965/v1 (2023).
29. Bastogne, T. Quality-by-design of nanopharmaceuticals – a state of the art. *Nanomedicine* 13, 2151–2157 (2017).
30. Đorđević, S., Medel, M., Conejos-Sánchez, I. *et al.* Current hurdles to the translation of nanomedicines from bench to the clinic. *Drug Deliv. Transl. Res.* 12, 500–525 (2021).
31. Molnar, C., Freiesleben, T., König, G. *et al.* Relating the partial dependence plot and permutation feature importance to the data generating process. in *Machine Learning and Knowledge Discovery in Databases* 456–479 (Springer, 2023).
32. Kaneko, H. Cross-validated permutation feature importance considering correlation between features. *Anal. Sci. Adv.* 3, 278–287 (2022).
33. Schaduangrat, N., Lampa, S., Simeon, S. *et al.* Towards reproducible computational drug discovery. *J. Cheminform.* 12, 40 (2020).
34. Ye, Z., Yang, W., Yang, Y. & Ouyang, D. Interpretable machine learning methods for in vitro pharmaceutical formulation development. *Food Frontiers* 2, 195–207 (2021).
35. Liu, G., Lu, D. & Lu, J. Pharm-AutoML: An open-source, end-to-end automated machine learning package for clinical outcome prediction. *CPT Pharmacometrics Syst. Pharmacol.* 10, 478–488 (2021).
36. Bobadilla, A. V. P., Schmitt, V., Maier, C. S. *et al.* Practical guide to SHAP analysis: Explaining supervised machine learning model predictions in drug development. *Clin. Transl. Sci.* 17, e13712 (2024).
37. Hoseini, B., Jaafari, M. R., Golabpour, A. *et al.* Application of ensemble machine learning approach to assess the factors affecting size and polydispersity index of liposomal nanoparticles. *Sci. Rep.* 13, 17894 (2023).
38. Hond, A. d., Shah, V., Kant, I. *et al.* Perspectives on validation of clinical predictive algorithms. *npj Digit. Med.* 6, 83 (2023).
39. Shen, C., Zhang, M., Lu, M. *et al.* Machine learning empowered formulation design, optimization and characterization of nanoparticulate drug delivery systems: Current applications, challenges, and future perspectives. *Acta Pharm. Sin. B* 16, 665–685 (2025).
40. Ortiz-Perez, A., Tilborg, D. v., Meel, R. v. d. *et al.* Machine learning-guided high throughput nanoparticle design. *Digit. Discovery* 3, 1280–1291 (2024).

41. Parker, A., Opletal, G. & Barnard, A. S. Classification of platinum nanoparticle catalysts using machine learning. *J. Appl. Phys.* 128, 144301 (2020).
42. Almansour, K. & Alqahtani, A. S. Utilization of machine learning approach for production of optimized PLGA nanoparticles for drug delivery applications. *Sci. Rep.* 15, 8840 (2025).
43. Bao, Z., Yung, F., Hickman, R. J. *et al.* Data-driven development of an oral lipid-based nanoparticle formulation of a hydrophobic drug. *Drug Deliv. Transl. Res.* 14, 1872–1887 (2023).
44. Glaubitz, C., Rothen-Rutishauser, B., Lattuada, M. *et al.* Designing the ultrasonic treatment of nanoparticle-dispersions via machine learning. *Nanoscale* 14, 12940–12950 (2022).
45. Jones, D., Ghandehari, H. & Facelli, J. C. A review of the applications of data mining and machine learning for the prediction of biomedical properties of nanoparticles. *Comput. Methods Programs Biomed.* 132, 93–103 (2016).
46. Seegobin, N., Abdalla, Y., Li, G. *et al.* Optimising the production of PLGA nanoparticles by combining design of experiment and machine learning. *Int. J. Pharm.* 667, 124905 (2024).
47. Ortiz-Perez, A., Tilborg, D. v., Meel, R. v. d. *et al.* Machine learning-guided high throughput nanoparticle design. *ChemRxiv* Preprint at https://doi.org/10.26434/chemrxiv-2023-sqb5c (2023).
48. Sato, S., Sano, S., Muto, H. *et al.* Understanding the manufacturing process of lipid nanoparticles for mRNA delivery using machine learning. *Chem. Pharm. Bull.* 72, 529–539 (2024).
49. Zulbeari, N., Wang, F., Mustafova, S. S. *et al.* Machine learning strengthened formulation design of pharmaceutical suspensions. *Int. J. Pharm.* 668, 124967 (2024).
50. Hanari, N., Mihandoost, S. & Rezvantalab, S. Intelligence prediction of microfluidically prepared nanoparticles. *Sci. Rep.* 15, 37512 (2025).
51. Zhang, Z., Xiang, Y., Laforêt, J. *et al.* TuNa-AI: A hybrid kernel machine to design tunable nanoparticles for drug delivery. *ACS Nano* 19, 33288–33296 (2025).
52. Kaur, J., Kaur, H., Kumar, R. *et al.* An AI-integrated approach to nano-based drug delivery systems: Advances in targeting and smart nano-carriers. in *Proceedings of ICICIS* 1–7 (IEEE, 2025).
53. Rahdar, A., Fathi-karkan, S. & Shirzad, M. Integrating machine learning and physics-based modeling for predictive design of gemcitabine-loaded nanocomposites. *Sci. Rep.* 16, 6268 (2026).

Table 1. Dataset structure used for independent AI modeling

Variable/response	Role	Type/coding	Experimental range or values	Unit
Lecithin:chitosan molar ratio	Input variable	Continuous	10–40	Molar ratio
Drug amount	Input variable	Continuous	10–100	mg
Mixing time	Input variable	Continuous	5–30	min
Heating condition	Input variable	Binary categorical	0 = absent; 1 = present	Coded
Mixing method	Input variable	Binary categorical	0 = mechanical stirring; 1 = sonication	Coded
Isopropyl myristate condition	Input variable	Binary categorical	0 = absent; 1 = present	Coded
Particle size	Prediction target	Continuous response	131.8–499.9	nm
Polydispersity index	Prediction target	Continuous response	0.132–0.400	Dimensionless
Entrapment efficiency	Prediction target	Continuous response	72.28–97.09	%
Total formulation runs	Dataset structure	Screening + optimization	13 screening runs + 16 optimization runs = 29 total runs	Runs

The dataset was extracted from the published lecithin/chitosan nanoparticle QbD study and used for independent machine-learning reanalysis [5].

Table 2. Best internally validated AI model for each critical quality attribute

Response	Best internally validated model	Validation method	R^2	MAE	RMSE	Unit of error
Particle size	XGBoost depth3 lr0.06	LOOCV	0.926	17.09	27.52	nm
Polydispersity index	Extra Trees leaf1 all	LOOCV	0.695	0.0281	0.0379	Dimensionless
Entrapment efficiency	KNN k2 distance	LOOCV	0.938	1.16	1.72	%

Note: LOOCV, leave-one-out cross-validation; MAE, mean absolute error; RMSE, root mean squared error.

Table 3. Final model-selection summary using global validation and optimized-checkpoint agreement

Response	Selection role	Selected model	R^2	MAE	RMSE	Optimized-checkpoint AI prediction	AI absolute error at checkpoint	Checkpoint interpretation
Particle size	Primary LOOCV-best model	XGBoost depth3 lr0.06	0.926	17.09	27.52	194.395	32.994	RSM closer at checkpoint
Particle size	Checkpoint-compatible model	Gaussian Process noise0.01	0.874	22.19	35.80	162.190	0.789	AI closer at checkpoint
Polydispersity index	Primary LOOCV-best model	Extra Trees leaf1 all	0.695	0.0281	0.0379	0.19295	0.01105	AI closer at checkpoint
Polydispersity index	Checkpoint-compatible model	Random Forest leaf3 all	0.569	0.0362	0.0451	0.20439	0.00039	AI closer at checkpoint
Entrapment efficiency	Primary LOOCV-best model	KNN k2 distance	0.938	1.16	1.72	95.564	1.496	RSM closer at checkpoint
Entrapment efficiency	Checkpoint-compatible model	KNN k2 distance	0.938	1.16	1.72	95.564	1.496	RSM closer at checkpoint

Table 4. Comparison of experimental, reported QbD/RSM, and independent AI predictions at the optimized formulation checkpoint

Response	Experimental observed value	Reported QbD/RSM prediction	Selected AI prediction	QbD/RSM absolute error	AI absolute error	AI models closer than QbD/RSM, n/N	Closer method for selected comparison
Particle size (nm)	161.401	152.597	162.190	8.804	0.789	10/105	Independent AI
Polydispersity index	0.204	0.172	0.2044	0.032	0.0004	88/105	Independent AI
Entrapment efficiency (%)	97.060	96.016	95.564	1.044	1.496	19/105	QbD/RSM

Table 5. Permutation feature importance for selected independent AI models

Response	Feature	Importance mean	Importance SD	Rank
Particle size	Drug amount	44.9515	5.2031	1
Particle size	Lecithin:chitosan molar ratio	44.4747	7.4513	2
Particle size	Mixing time	44.0505	8.6473	3
Particle size	Mixing method	3.8624	1.3275	4
Particle size	Heating condition	3.8104	1.0539	5
Particle size	Isopropyl myristate condition	2.0617	0.6219	6
Polydispersity index	Lecithin:chitosan molar ratio	0.04189	0.00792	1
Polydispersity index	Drug amount	0.00348	0.00157	2
Polydispersity index	Heating condition	0.00127	0.00041	3
Polydispersity index	Isopropyl myristate condition	0.00100	0.00044	4
Polydispersity index	Mixing method	0.00018	0.00018	5
Polydispersity index	Mixing time	0.00006	0.00011	6
Entrapment efficiency	Lecithin:chitosan molar ratio	1.9010	0.4077	1
Entrapment efficiency	Mixing method	1.8708	0.6285	2
Entrapment efficiency	Drug amount	1.8066	0.5353	3
Entrapment efficiency	Mixing time	0.8998	0.3006	4
Entrapment efficiency	Isopropyl myristate condition	0.5163	0.2042	5
Entrapment efficiency	Heating condition	0.1298	0.0692	6

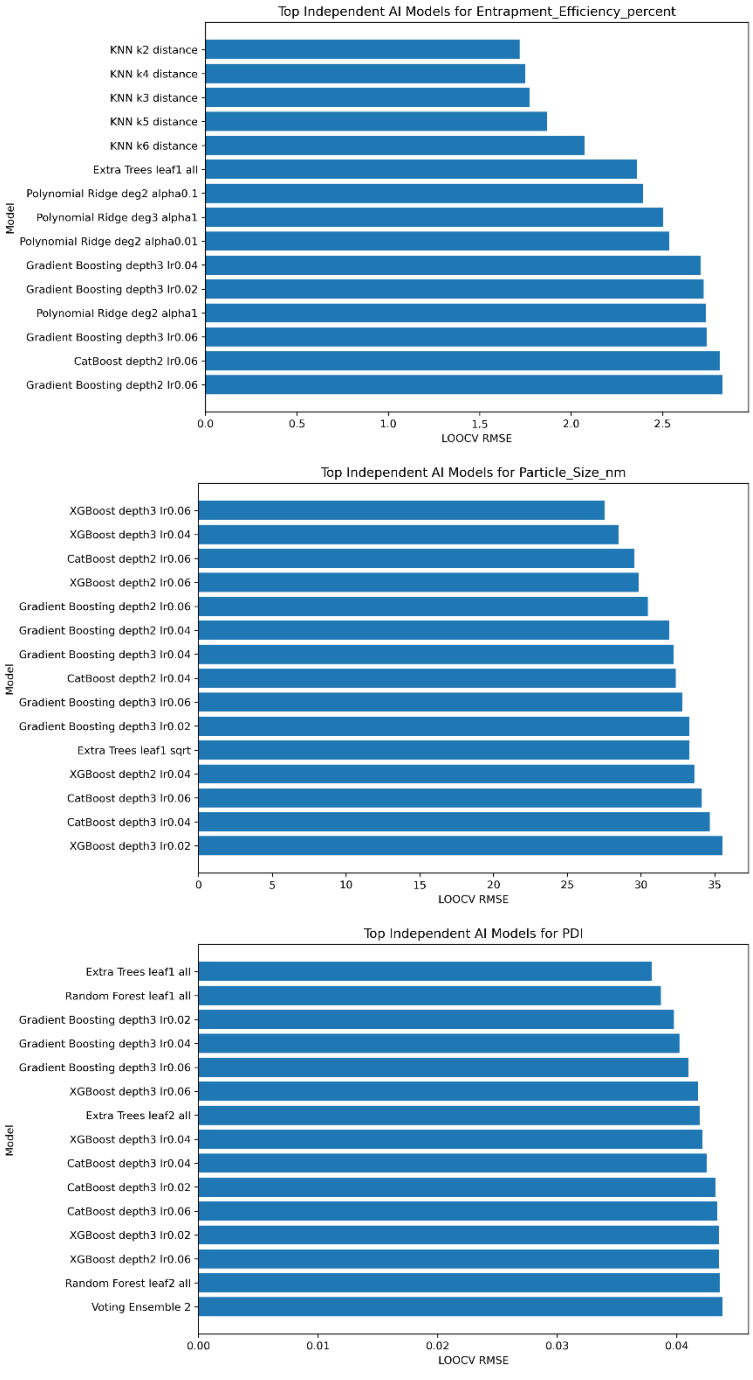


Fig. 1. Ranking of independent AI models by cross-validated prediction error

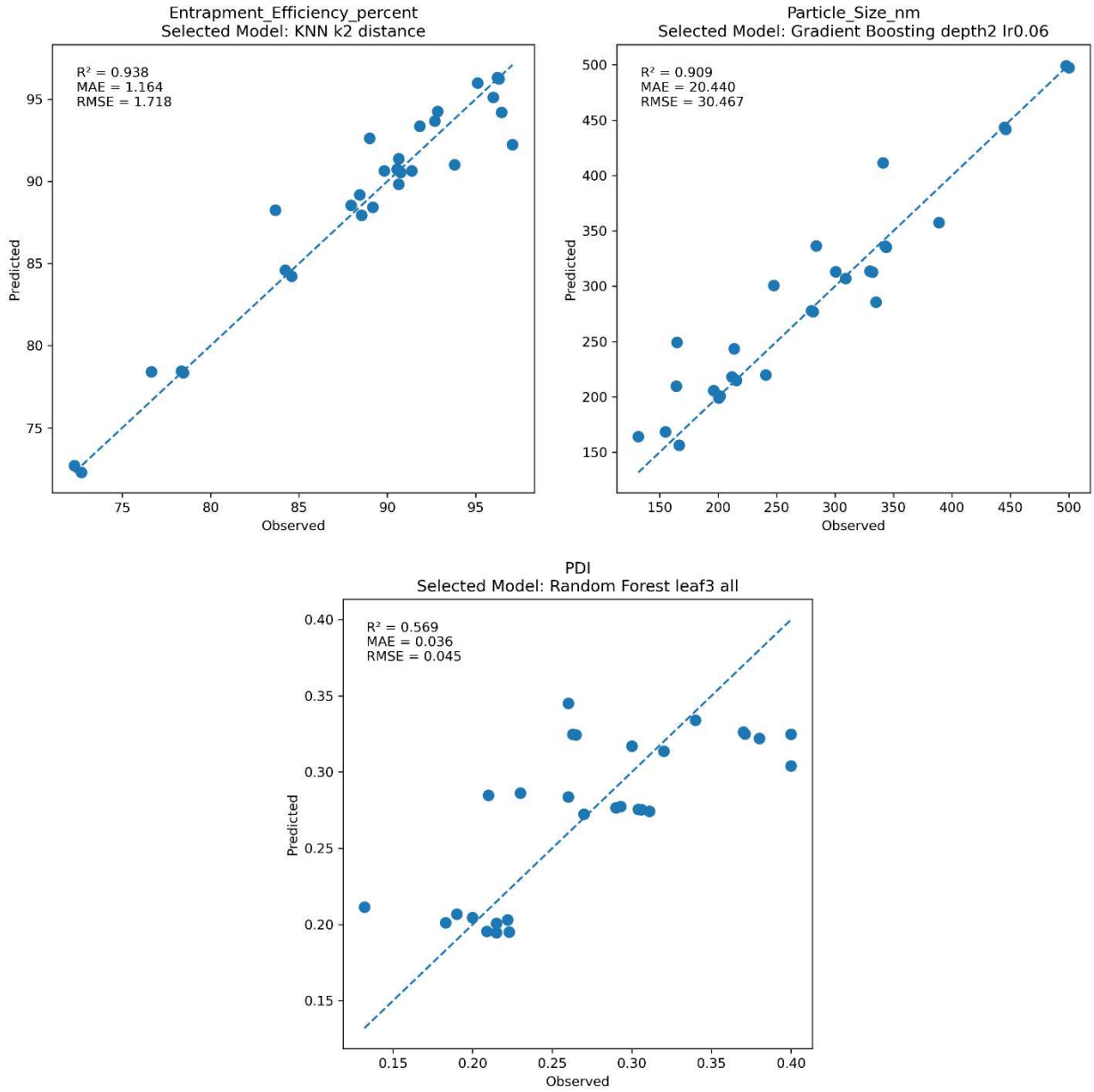


Fig. 2. Observed versus predicted plots for selected independent AI models

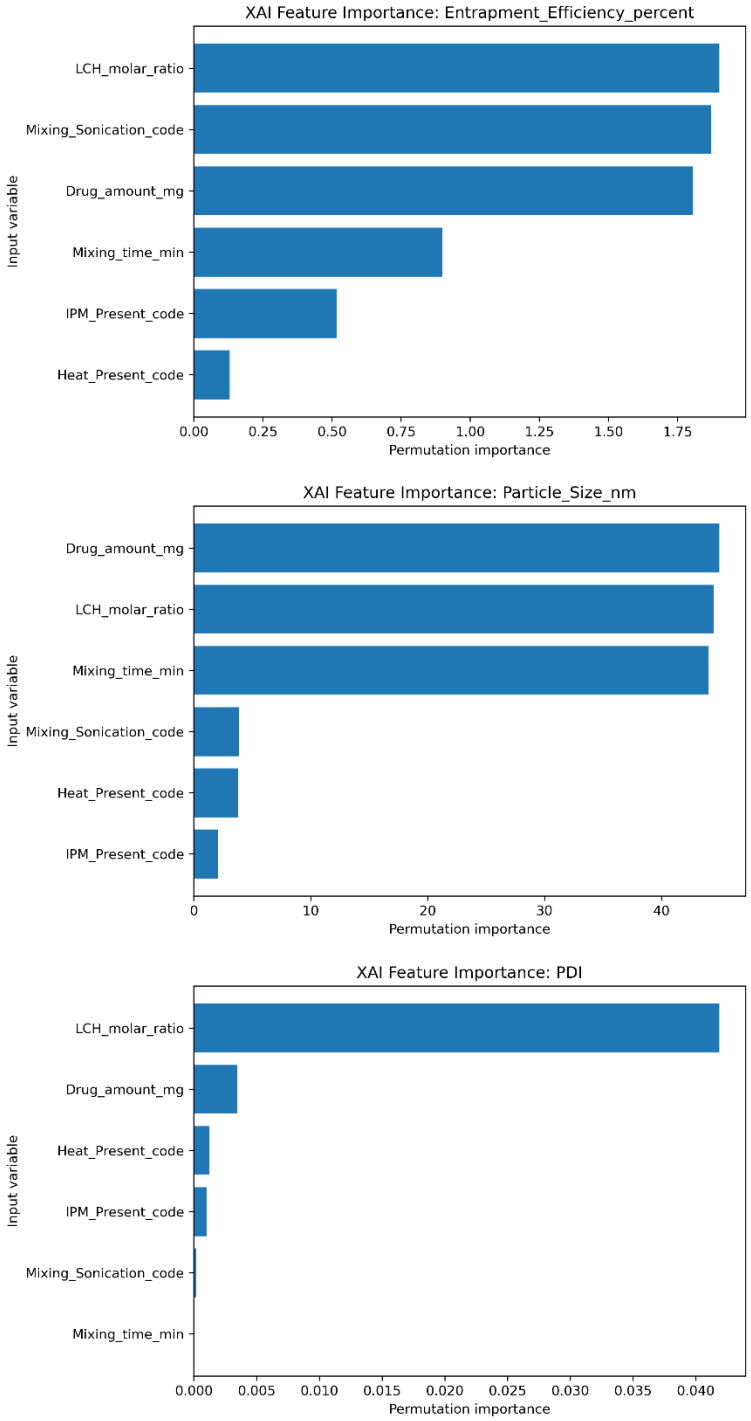
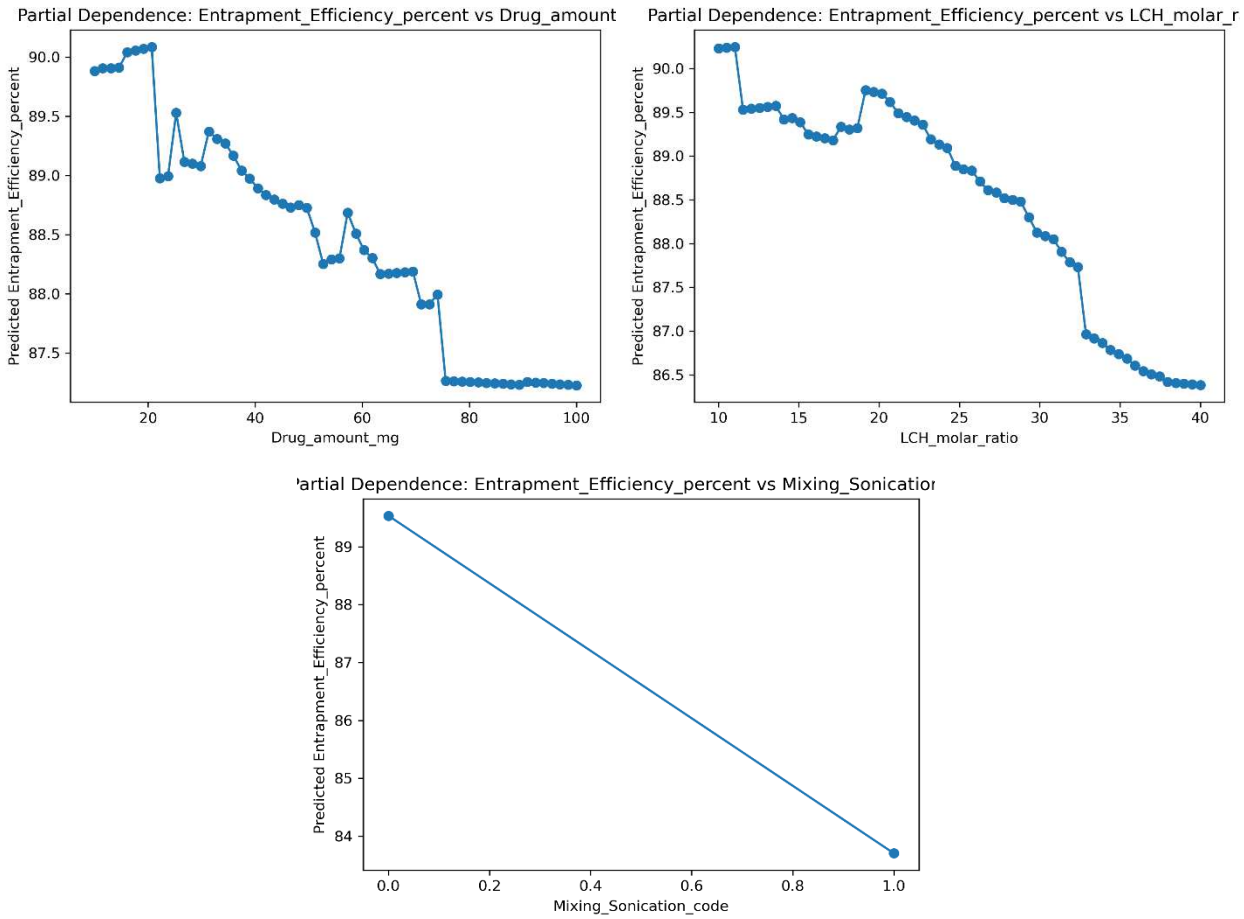


Fig. 3. Permutation feature importance of selected AI models



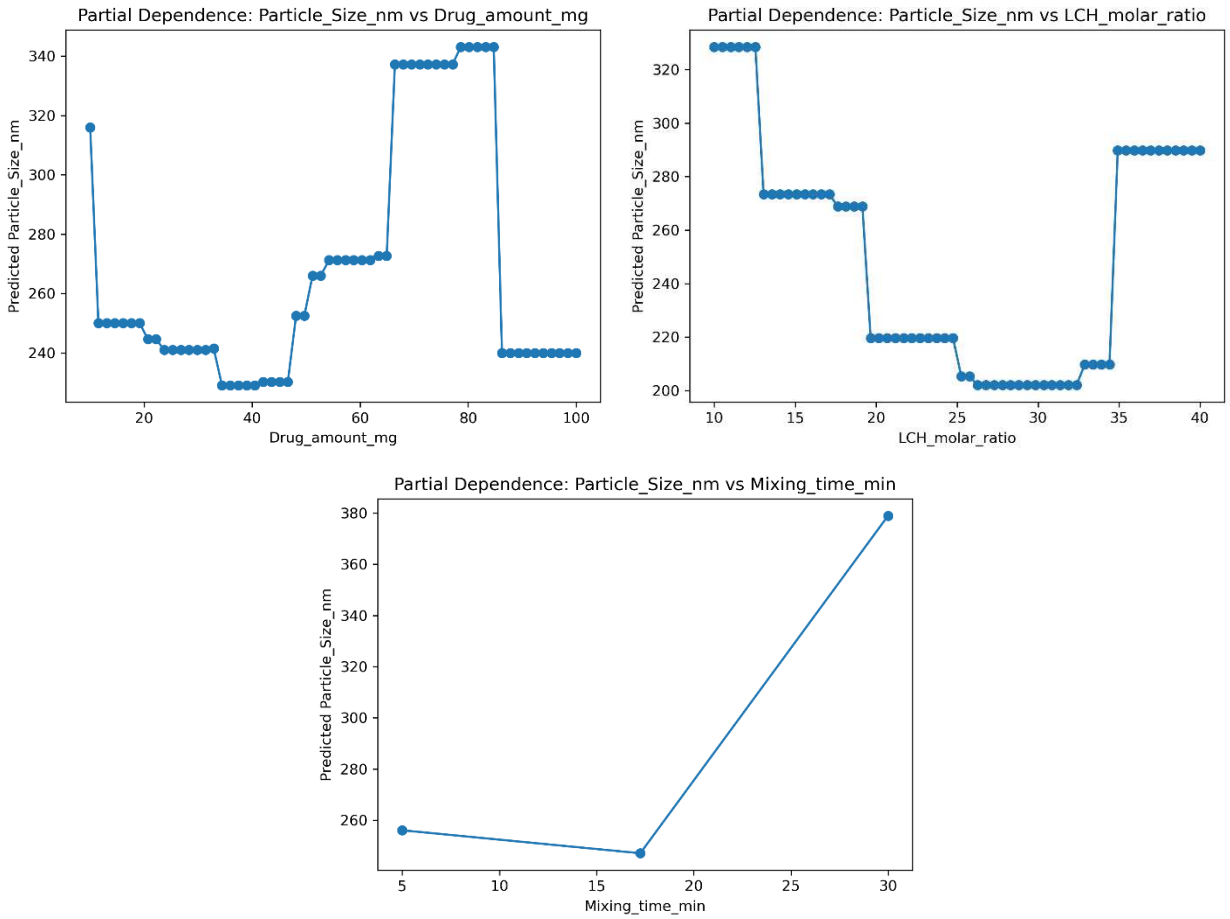
816

817

818

819 **Fig. 4a. Partial dependence analysis of key formulation and Entrapment Efficiency**

820



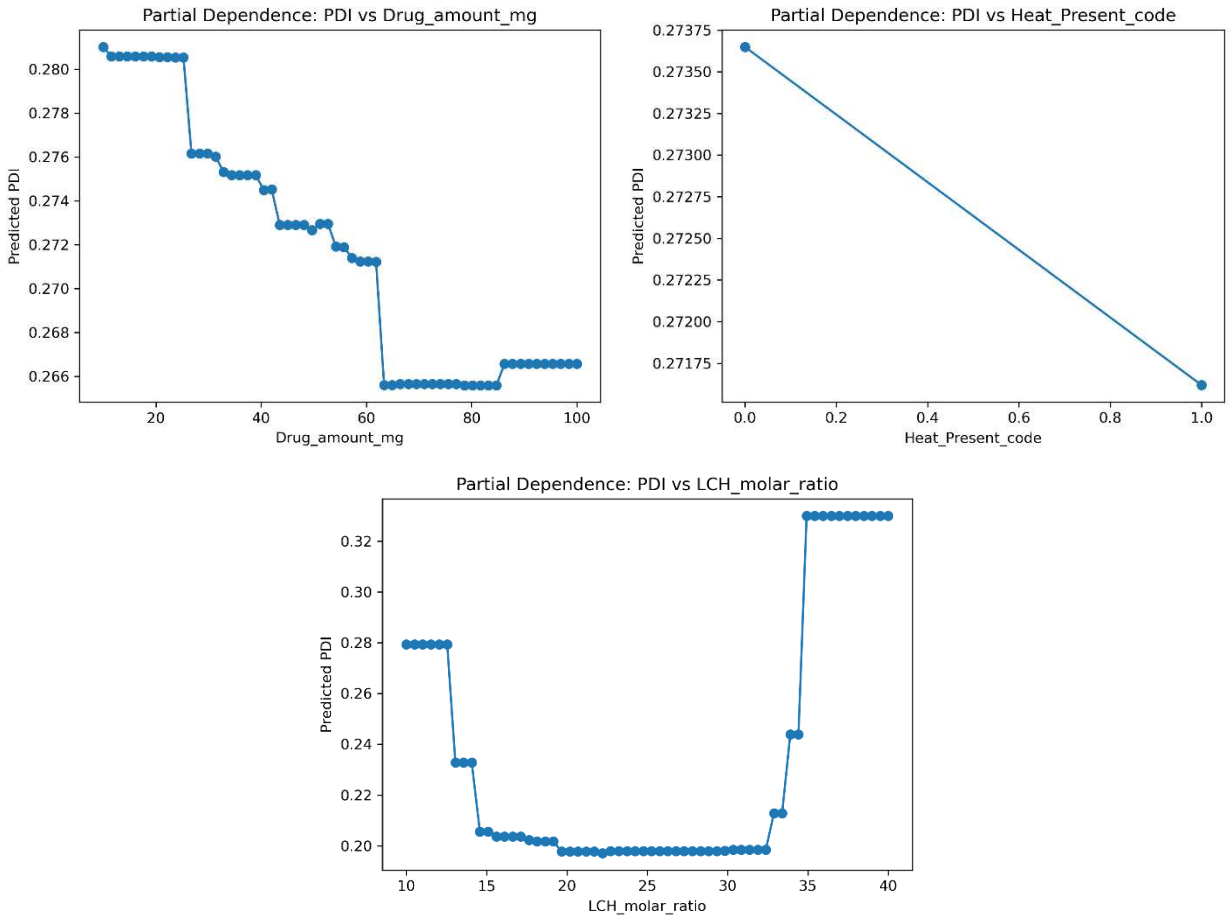
821

822

823

824 **Fig. 4b. Partial dependence analysis of key formulation and particle size**

825



826

827

828 **Fig. 4c. Partial dependence analysis of key formulation and PDI**

829

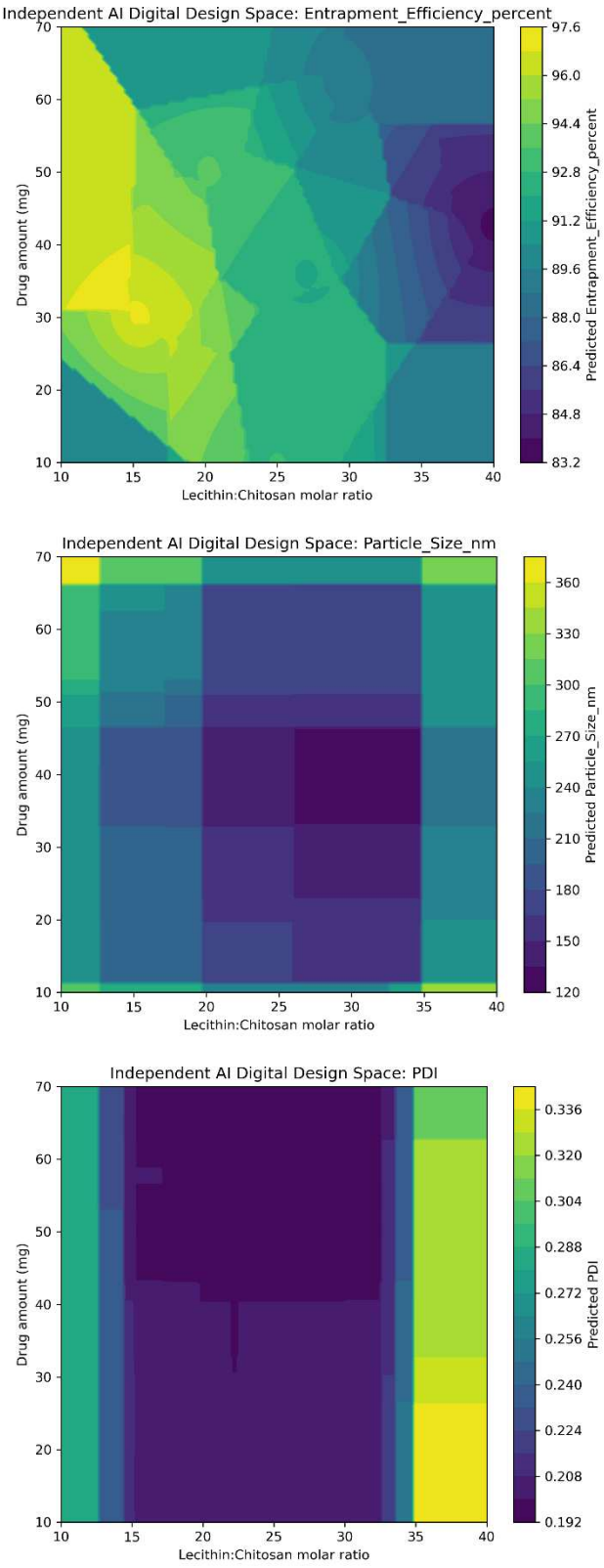
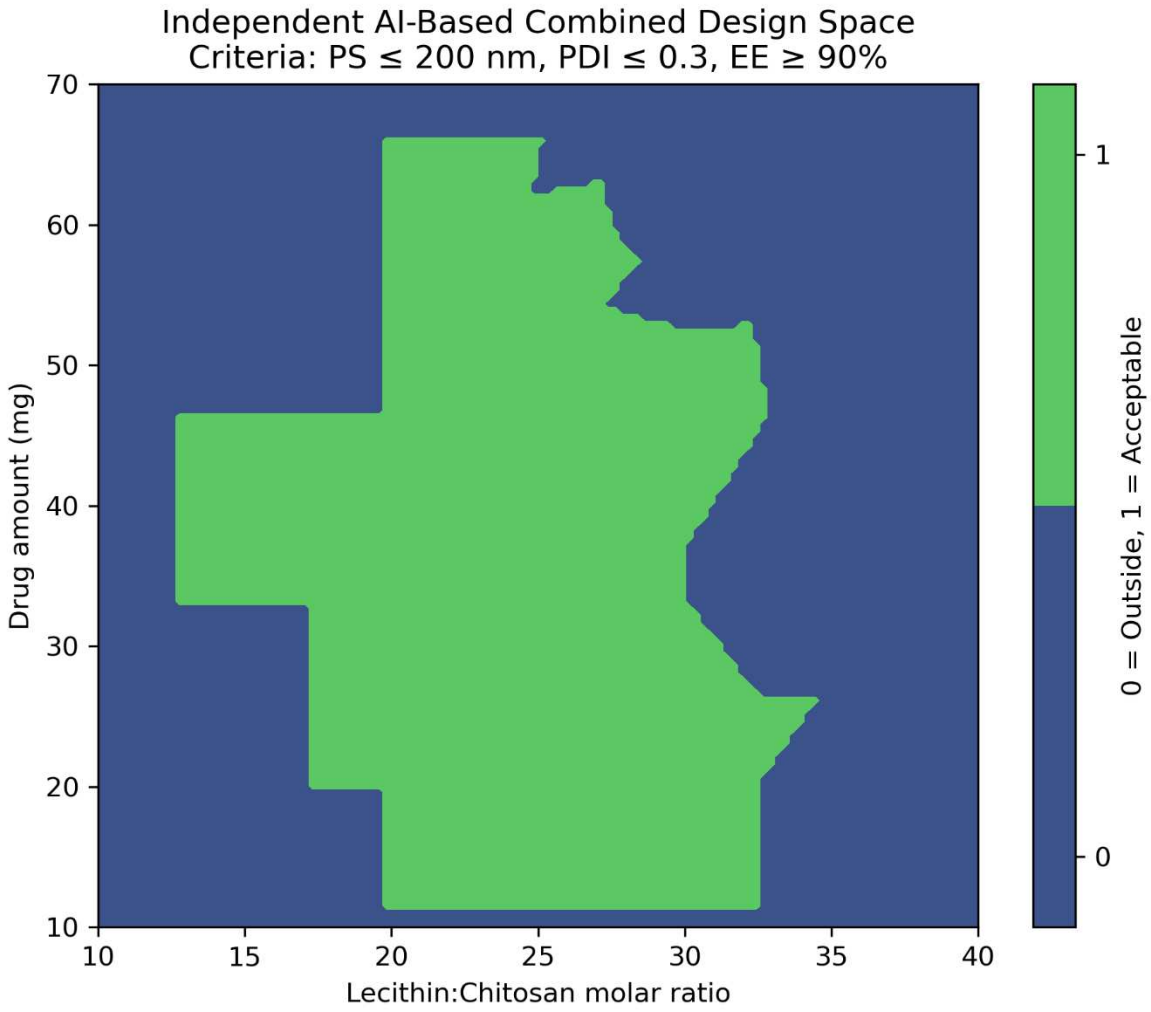


Fig. 5. AI-based response maps for lecithin/chitosan nanoparticles



835

836 **Fig. 6. Combined predictive design space generated by independent AI**

837

Acknowledgements

The authors acknowledge the original investigators of the published lecithin/chitosan nanoparticle study, whose reported formulation data provided the basis for the present secondary computational reanalysis. The authors also acknowledge their respective institutions for academic support during manuscript preparation.

Author Contributions

R.D. and N.S. conceptualized the study, developed the overall QbD–explainable AI framework, supervised the computational interpretation, and contributed to manuscript preparation. S.S. contributed to data extraction, dataset organization, literature review, formulation-related interpretation, and manuscript drafting. N.S. performed the machine-learning workflow, model comparison, optimized-checkpoint analysis, explainable AI interpretation, and digital design space mapping. S.T. contributed to methodological review, interpretation of computational findings, and critical revision of the manuscript. P.S.S. assisted in literature support, data checking, and preparation of tables and figures. P.C. contributed to scientific review, editing, and refinement of the discussion. All authors reviewed and approved the final version of the manuscript.

Funding

No external funding was received for this study.

Declaration of Competing Interests

The authors declare that they have no known competing financial interests or personal relationships that could have appeared to influence the work reported in this paper.

Ethics Statement

This study was based exclusively on a previously published formulation dataset and did not involve human participants, animals, clinical specimens, patient records, or new wet-laboratory experimentation. Therefore, ethics committee approval was not required.

Data Availability

The study used formulation data extracted from a previously published lecithin/chitosan nanoparticle QbD study cited in the manuscript. The processed dataset, model-output tables, checkpoint-comparison results, and model-zoo summary are provided in the supplementary material.

Code Availability

The Python notebook used for data preprocessing, model training, leave-one-out cross-validation, optimized-checkpoint comparison, explainable AI analysis, and predictive design space mapping is available from the corresponding author upon reasonable request.

Supplementary Material Statement

Supplementary material accompanies this manuscript. Supplementary Table S1 contains the complete independent AI model-zoo performance and optimized-checkpoint comparison for all tested model-response combinations. Additional supporting files include processed model outputs and figures related to model ranking, observed versus predicted plots, feature importance, partial dependence analysis, and predictive design space mapping.